

Article

## The Role of Infragravity Waves in Near-Bed Cross-Shore Sediment Flux in the Breaker Zone

Samantha Kularatne <sup>†</sup> and Charitha Pattiaratchi <sup>†,\*</sup>

School of Civil, Environmental and Mining Engineering and The UWA Oceans Institute,  
The University of Western Australia, 35 Stirling Highway, Crawley 6009, Australia;  
E-Mail: chari.pattiaratchi@uwa.edu.au

<sup>†</sup> These authors contributed equally to this work.

\* Author to whom correspondence should be addressed; E-Mail: chari.pattiaratchi@uwa.edu.au;  
Tel.: +61-8-6488-3179; Fax: +61-8-6488-1015.

*Received: 20 December 2013; in revised form: 19 May 2014 / Accepted: 6 June 2014 /*

*Published: 19 August 2014*

---

**Abstract:** Results from a series of field experiments, conducted to investigate the influence of infragravity waves (from wave groups), ripple type and location relative to the breaker line on cross-shore suspended sediment flux close to the sea bed in nearshore environments, are presented. The field data were collected from Cable Beach (Broome) and Mullaloo Beach in Western Australia and Chilaw in Sri Lanka. These beaches experience different incident wave, tidal and morphological conditions, with Cable Beach having a 10-m spring tidal range, whilst the other two beaches have tidal ranges <1.0 m. Measurements included simultaneous records of surface elevation, two-dimensional horizontal current velocities and suspended sediment concentrations, together with half-hourly observations of the seabed topography. Although most of the data sets were obtained just outside of the surf zone, a few results from inside of the surf zone were also included. A significant correlation between wave groups and suspended sediment concentration was found at all of the measurement sites, either with or without bed ripples. The direction and magnitude of cross-shore suspended sediment flux varied with location with respect to the breaker line; however, other parameters, such as bed ripples and velocity skewness, could have influenced this result. In Broome, where the measurement location with respect to the breaker line varied with the tidal cycle, the cross-shore sediment flux due to swell waves

was shoreward inside and just outside of the surf zone and seaward farther offshore of the breaker line. Further, sediment flux due to swell waves was onshore when the seabed was flat and offshore over post-vortex ripples. Sediment flux due to swell waves was onshore when the normalised velocity skewness towards the shore was high (positive); the flux was offshore when the skewness was lower, but positive, suggesting the influence of other parameters, such as ripples and grain size. The net cross-shore sediment flux was onshore when the Dean number was less than 1.67 and offshore when the Dean number was greater than 1.67. Nevertheless, the Dean number did not account for the influence of ripples or velocity skewness. The cross-shore sediment flux at the infragravity frequency was mainly offshore outside of the surf zone, whereas it varied between onshore and offshore inside of the surf zone.

**Keywords:** cross-shore sediment transport; sediment re-suspension; bed ripples; velocity skewness; Dean number; wave groups; group-bound long wave

---

## 1. Introduction

With rising global sea levels and rapidly increasing population densities along coastal stretches, coastal stability has become a major issue for coastal communities and managers. The accurate prediction of sediment transport in nearshore environments is one of the most complex challenges coastal researchers encounter. However, although nearshore sediment transport mainly occurs in the alongshore direction, the cross-shore transport is dominant in determining seasonal shoreline evolution and beach morphology [1–3]. Further, it has been noted that longshore transport is predominantly due to the mean motion (mean over several wave periods) [4], whereas a range of mean (tides, undertow and rip currents) and oscillatory components (wind waves, swell, wave groups and infragravity oscillations) drives cross-shore transport [5]. Each of these frequency components uniquely influences the direction and magnitude of cross-shore sediment flux under different conditions [6]. Therefore, an improved understanding of the processes of sediment re-suspension and flux due to the different oscillatory components is essential to predict cross-shore sediment transport and, thus, coastal stability, accurately.

The majority of previous studies revealed that the suspension of sediment, and, hence, the cross-shore sediment flux in nearshore regions, occurred in an event-like manner over timescales ranging from seconds (wind waves, swell) to minutes (wave groups or infragravity waves) [7–10]. These studies further indicated that suspension events that occurred in infragravity periods were much more pronounced than those at incident frequencies (wind waves, swell) [6,9–14]. Here, we define infragravity waves as those waves with periods ranging between 30 and 300 s, and in this paper, they were mainly generated through the presence of wave groups. This enhanced the assumption that wave groups are more capable than individual incident waves of suspending sediment particles from the bed. Vincent *et al.* [12] proposed that pronounced suspension events under infragravity wave periods were due to changes in ripple geometry during the passage of wave groups. However, higher suspension events at wave group frequencies have also been observed under flat bed conditions [15,16]. Osborne

and Greenwood [10] and Hanes and Huntley [9] explained that persistent turbulence, propagated by the larger waves of wave groups, could pump more sediment into the water column. From a series of experiments conducted in a large-scale wave research flume over rippled beds, Villard and Osborne [17] suggested that higher suspension events that occurred at the group frequency following larger waves of the group might be due to the coupling between antecedent vortices created by the larger waves and developing vortices created by the smaller waves, which followed the larger waves.

Observations of cross-shore sediment flux under different conditions and at various locations worldwide have revealed that the direction of cross-shore sediment flux under different frequency components is variable. Huntley and Hanes [9] found that for shoaling waves outside of the breaker zone, the cross-shore sediment flux was directed onshore at the incident wave frequencies (wind waves, swell) and offshore at lower frequencies (wave groups, infragravity waves). The shoreward sediment flux under incident waves as waves shoal was attributed to the increasing velocity skewness in the propagation direction [18,19]. The sediment suspended at infragravity (mainly due to wave groups) frequencies coupled with the offshore phase of the group-bound long wave [20] resulted in a net offshore sediment transport at those frequencies [21,22].

However, other investigators have documented cases where there was offshore flux of sediment at incident frequencies and *vice versa* for infragravity frequencies [15,23,24]. These deviations were assumed to be due to various factors, such as the presence of ripples [12,15,23,25,26], variation in wave energy (during a storm) [23], varying tide level [15] and grain size [27]. Further, the relative magnitudes and directions of these different frequency components could vary with the location of the measurements with respect to the breaker line [15,19,24,28], as well as the measurement height above the bed [29,30]. The different processes discussed above are those contributing to cross-shore sediment flux due to oscillatory fluid motion, and it should be noted that there are also mean flows that contribute to cross-shore sediment flux, such as undertow, rip currents and tidal currents. However, these processes are outside the scope of this paper.

Some results indicated that cross-shore flux under infragravity frequencies, corresponding to wave groups, was directed offshore outside of the breaker zone and onshore inside of the breaker zone [24]. The mean component of the sediment flux in the surf zone was mainly offshore below the wave trough level, because of the presence of undertow (bed return flow). The mean flow (zero frequency) component, however, was not considered in the present study. Nonetheless, the observations by Aagaard and Greenwood [24] emphasised the complexity involved in sediment transport processes in this highly dynamic region and, thus, the need for a better understanding of the factors influencing the magnitude and direction of cross-shore sediment transport.

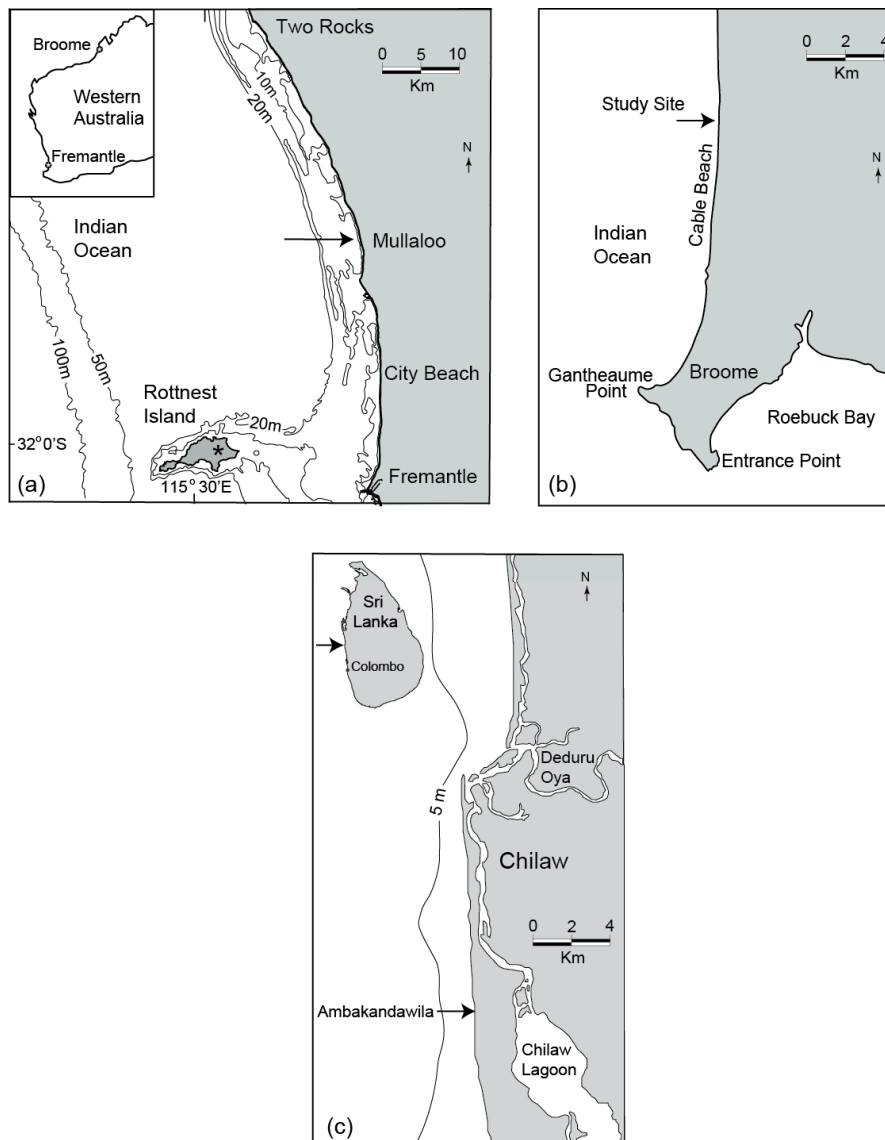
This paper describes results obtained through a series of field measurements (water surface elevation, horizontal current velocities and suspended sediment concentration) undertaken in different nearshore environments under various conditions, such as differing tide, grain size, bed geometry and cross-shore location. The aim of the experiments was to investigate the influence of infragravity waves (from wave groups), ripple type and location relative to the breaker line on cross-shore suspended sediment flux close to the sea bed in nearshore environments.

## 2. Methodology

### 2.1. Field Sites

Field measurements providing the basis for the present study were undertaken at several locations: Mullaloo Beach, south-western Australia (Figure 1a); Cable Beach, Broome, north-western Australia (Figure 1b); and Ambakandawila Beach, Chilaw, Sri Lanka (Figure 1c). These locations encompass a range of different incident wave conditions, tidal range and beach morphologies.

**Figure 1.** Location maps of the study sites. (a) Mullaloo Beach, Perth, Western Australia; (b) Cable Beach, Broome, Western Australia; (c) Ambakandawila Beach, Chilaw, Sri Lanka.



Mullaloo Beach in south-western Australia (Figure 1a) experiences diurnal micro-tidal conditions, with a maximum tidal range of 0.6 m [31]. The incident wave climate changes seasonally and is divided into three regimes: (1) summer sea breezes; (2) winter storms; and (3) swell-dominated periods between sea breezes (*i.e.*, during the morning in summer) and between the passage of frontal systems

during winter [32,33]. The latter regime is also dominated by the presence of wave groups and was the focus of this paper.

Cable Beach, in Broome, north-western Australia (Figure 1b), experiences a macro-tidal regime with a maximum spring tidal range of 9.8 m [34]. It is generally subject to low to medium energy swell conditions, with significant wave heights of 0.5–1.5 m [34].

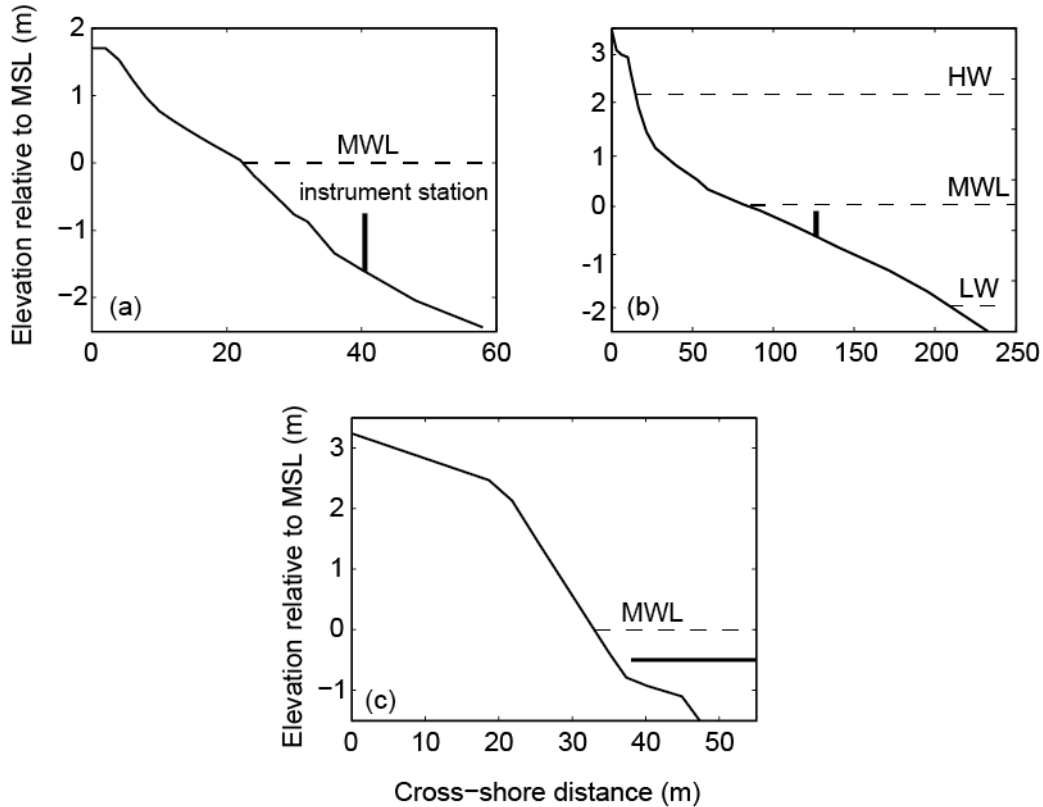
Ambakandawila Beach, located to the south of Chilaw, on the west coast of Sri Lanka (Figure 1c), experiences similar conditions to those of south-western Australia [35], but with a semi-diurnal tidal regime. The wave climate here could also be divided into three regimes, similar to those of south-western Australia. This site was chosen to compare with south-western Australia, which has a similar tidal range, but experiences a semi-diurnal tidal regime.

The measurements were conducted over different years: April (autumn), 1993, Mullaloo; January (summer), 1996, Chilaw; and August (winter), 1997, Broome. Details and the characteristics of these three beaches are listed on Table 1. At all locations, the measurements were undertaken at long, straight, exposed beaches, where there was the absence of nearshore reefs, islands or offshore/coastal structures in the vicinity, allowing for waves to be incident on the beach under only shoaling conditions. The field measurements reported here were obtained mainly during incident swell waves with peak wave periods of 14.2 s, 14.8 s and 14.9 s for Chilaw, Broome and Mullaloo, respectively. At the time of the measurements presented here, all of the beaches had a plane form and were not barred. The beach profiles, obtained during the measurements, at the different locations are presented in Figure 2. At Mullaloo and Chilaw, the conditions could be classified as reflective, since the beaches were relatively steep and the waves were seen breaking almost on the beach face, with a narrow surf zone. In contrast, Broome was dissipative, with a mild slope and wider surf zone. Surging breakers were observed at Mullaloo and Chilaw, whereas in Broome, the breaker type was spilling. The selected sites comprised a range of grain sizes: Mullaloo had medium to coarse sand with a median grain size ( $d_{50}$ ) of 0.28 mm; at Chilaw, the median grain size was 0.15 mm; and in Broome, the grains were fine with a median grain size of 0.11 mm. At the sites, the grain size showed little variation in the cross-shore direction.

**Table 1.** Characteristics of the field locations used in this study.

	<b>Mullaloo Beach, Perth, Western Australia</b>	<b>Cable Beach, Broome, Western Australia</b>	<b>Ambakandawila Beach, Chilaw Sri Lanka</b>
Date of experiment	April (autumn), 1993	August (winter), 1997	January (summer), 1996
Mean tidal range	0.6 m	9.8 m	0.8 m
Mean wave height	0.5–1.5 m	0.5–1.5 m	0.5–1.5 m
Peak Period	14.9 s	14.8 s	14.2 s
Breaker type	Surging	Spilling	Surging
Beach morphology	Reflective, non-barred	Dissipative, non-barred	Reflective, non-barred
Grain size ( $d_{50}$ )	0.28 mm	0.15 mm	0.11 mm
Measurement locations	Close to breaker zone	Inside and outside of the breaker zone depending on tidal state	Inside and outside of the breaker zone; instrument location changed during measurement period
Data collection rate	5 Hz	5 Hz	2 Hz

**Figure 2.** Cross-shore beach profiles. (a) Mullaloo Beach, Perth, Western Australia; (b) Cable Beach, Broome, Western Australia; (c) Ambakandawila Beach, Chilaw, Sri Lanka. In the Figure, HW, MWL and LW correspond to High Water, Mean Water Level and Low Water, respectively in terms of the tidal water levels.



*2.2. Field Data Collection*

At each site, the water surface elevation, two-dimensional horizontal current velocities and suspended sand concentration data were collected with the S-probe—An instrument station developed at the University of Western Australia [1,32]. The S-probe comprised a Paroscientific Digiquartz pressure sensor and a Neil Brown ACM2 acoustic current meter, together with three D & A Instrument Company optical backscatter turbidity sensors (OBS-3 model). The pressure sensor was located 0.35 m above the seabed. The current meter recorded the two-dimensional horizontal velocity (0.20 m), and the OBS sensors recorded the sediment concentration 0.050, 0.125 and 0.275 m above the seabed). However, only the data from the OBS at 0.05 m were used in this paper (due to the continuous data available at that height at all of the locations), and hence, the sediment flux discussed refers to the flux close to the seabed.

The cross-shore current velocity was measured at one vertical point (0.20 m), as it is widely considered that the velocities under oscillatory flow in shallow water remain constant over the depth, except within the narrow bottom boundary layer [6,24,36].

The sampling frequency used at Chilaw was 2 Hz; at Mullaloo and Broome it was 5 Hz. At Mullaloo, the measurements were conducted just offshore of the breaker zone (defined visually by where the waves were breaking), where the presence of wave groups could be observed with larger waves breaking offshore of the instrument. At Chilaw, the instrument station was moved back and forth around the

observed breaker line, with measurements obtained inside and outside of the breaker zone. In Broome, where the tidal range was high, the instrument station location varied with respect to the breaker line following the tidal movement. All of the measurements from Broome presented in this paper were conducted around high tide (morning and early afternoon) before the onset of the sea breeze. In Broome, the bed forming near the instrument station was also visually observed at half-hourly intervals using a snorkel and mask (see also [34]).

The majority of measurements were conducted during calm wind conditions (usually in the morning before the onset of the sea breeze), because the waves were swell-dominated, which was ideal for pronounced wave groups.

Seabed profiles were surveyed using a total station, and sediment samples, collected from the field sites, were used to determine the median grain size and to calibrate the OBSs. The OBSs were calibrated following the method explained in Ludwig and Hanes [37]. Additional details of the field measurements can be found in [32,34,35].

### 2.3. Data Analysis Techniques

All of the time series records, comprising surface elevation, cross-shore current velocity and suspended sediment concentration, were subjected to power and co-spectral analysis through digital Fourier transforms [38]. Each data record was divided into a series comprising of 8192 data points (~27 and ~68 min at 5 and 2 Hz, respectively), and then, each set was divided into 16 equal segments for the segment average method [38]. The number of degrees of freedom used was 32. Shorter data sets were used, especially for Broome, to avoid the influence of the tidal cycle. The 95% confidence interval calculated for all of the spectra presented in this paper indicated that the upper and lower confidence limits were 1.75- and 0.65-times the spectral estimates, respectively. The 95% confidence interval in the phase spectrum at the major frequency components were calculated using the coherence estimates [39] to determine the statistical significance of the major co-spectral peaks [15,24].

Time series records of the wave groupiness envelope, cross-shore current velocity and suspended sediment concentration were compared to investigate the effect of wave groupiness on sediment re-suspension. The modulus of the cross-shore current record was low-pass-filtered at 0.02 Hz to compute the groupiness envelope [40].

### 2.4. The Dean Number

The Dean number [41], being the ratio of a particle settling time to the wave period, can be used to predict the direction of the cross-shelf sediment flux. Here, it is considered that sediment is suspended in the water through the passage of a wave. If the sediment has a relatively higher fall velocity, then it would settle onto the sea bed on the onshore movement of the wave cycle, resulting in net onshore transport. In contrast, if the settling velocity is relatively low, it would settle onto the seabed on the offshore movement of the wave cycle, resulting in net offshore transport. The Dean number ( $D$ ) is given by:

$$D = \frac{\beta H_s}{w_s T_p} \quad (1)$$

where  $H_s$  is the significant wave height,  $w_s$  is the particle settling velocity,  $T_p$  is the peak period obtained from the spectrum of cross-shore current velocity and  $\beta$  is a constant ( $\approx 0.3$ ). Dean and Dalrymple [42] showed that the suspended sediment transport was onshore when:

$$D < \frac{1}{2\beta} \tag{2}$$

suggesting that the sediment flux should be onshore when  $D < 1.67$  and offshore when  $D > 1.67$ .

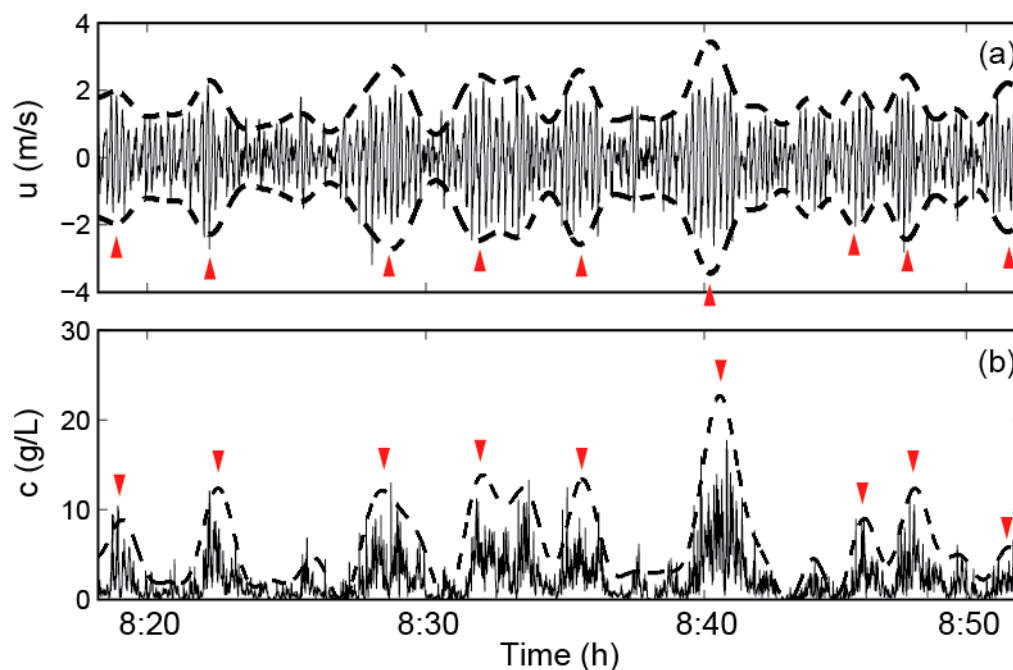
### 3. Results

Section 3.1 presents the relationship between suspended sediment concentration and wave groups. An analysis of cross-shore suspended sediment flux in the frequency domain is presented in Section 3.2. The cross-shore sediment flux results for shoaling, non-breaking waves over a flat bed are included in Section 3.2.1. Section 3.2.2 shows the temporal variability of cross-shore suspended sediment flux with the tidal cycle, and Section 3.2.3 compares the cross-shore sediment flux results obtained under breaking and broken waves. Finally, the results of the variation between the Dean number and the net cross-shore suspended sediment flux are presented in Section 3.2.4.

#### 3.1. Sediment Resuspension

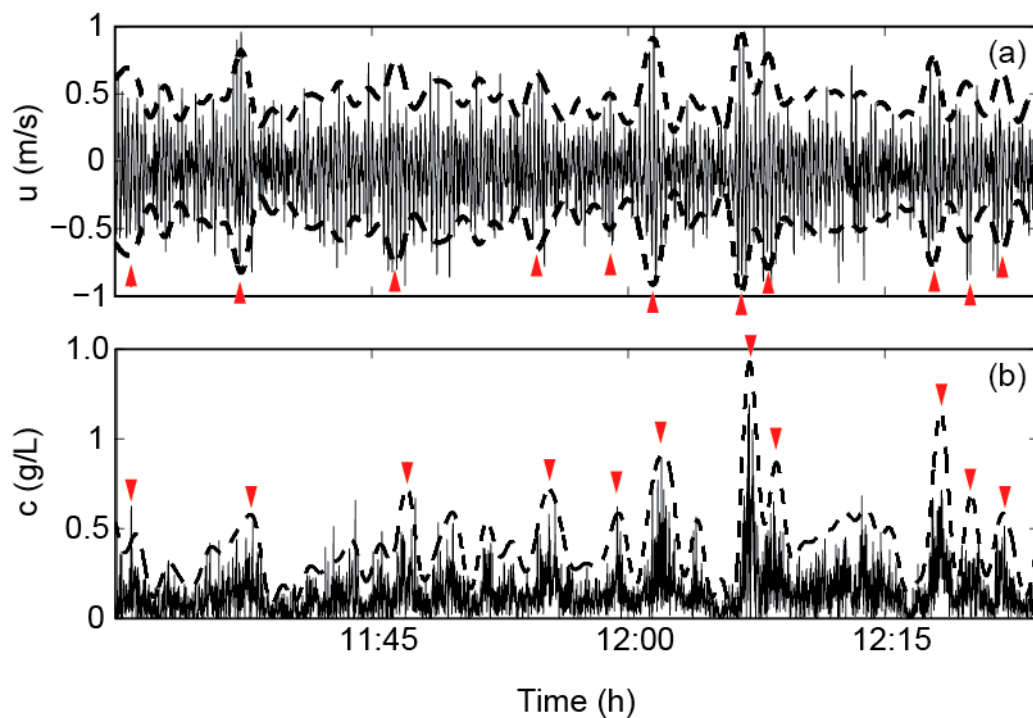
The time series records of the cross-shore current velocity ( $u$ ) at 0.20 m and of the suspended sediment concentration ( $c$ ) at 0.05 m from the bed obtained from Mullaloo Beach showed a strong correlation between the passing of wave groups and pronounced suspension events (Figure 3).

**Figure 3.** Time series of (a) cross-shore current velocity  $u$  ( $z = 0.25$  m; solid line) and the envelope function of  $u$  (thick, dashed lines); and (b) suspended sediment concentration  $c$  ( $z = 0.05$  m; solid line) and low-pass-filtered  $c$  (thick, dashed line) (just outside of the breaker line, over a flat bed, Mullaloo Beach, Western Australia).



Similar time series records obtained around high tide in swell-dominated conditions in Broome showed the same pattern: higher suspension events occurred as wave groups passed (Figure 4). The instrument station was ~110 m offshore of the moving breaker line; the seabed was covered with two-dimensional permanent post-vortex ripples with ripple heights of about 0.005 m and a spacing of 0.06–0.08 m. This trend of higher suspension events coinciding with passing wave groups was observed at all sites (data not shown) whenever pronounced wave groups were present, either in the presence or absence of ripples.

**Figure 4.** Time series of (a) cross-shore current velocity  $u$  ( $z = 0.25$  m; solid line) and the envelope function of  $u$  (thick, dashed lines); and (b) suspended sediment concentration  $c$  ( $z = 0.05$  m; solid line) and low-pass-filtered  $c$  (thick, dashed line) (shoaling waves over two-dimensional permanent post-vortex ripples, Cable Beach, Broome, Western Australia).



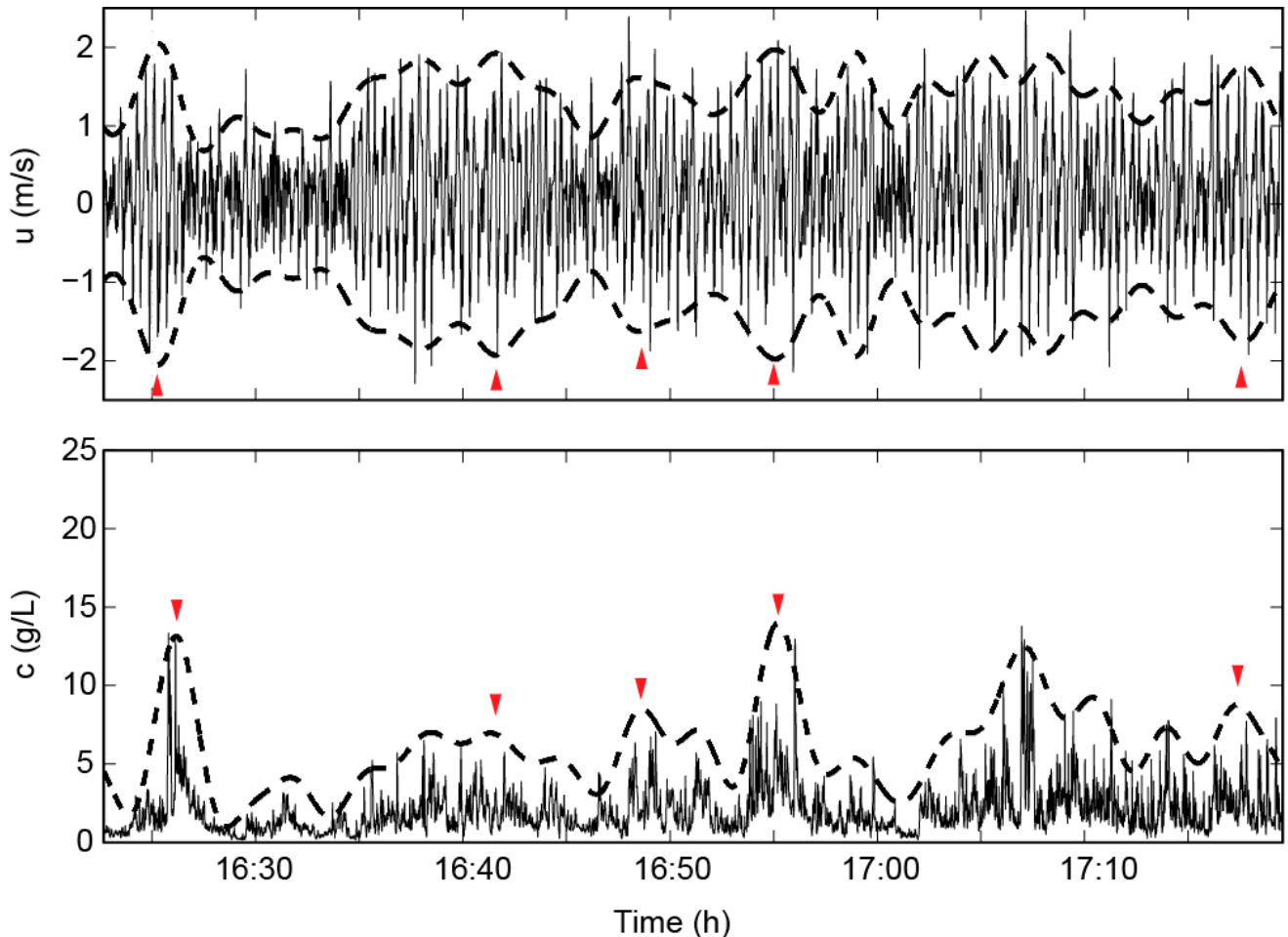
A similar result is also observed at Ambakandawila between the passing of wave groups and pronounced suspension events (Figure 5).

### 3.2. Cross-Shore Sediment Flux

#### 3.2.1. Shoaling, Non-Breaking Waves over a Flat Bed

Spectral analyses were undertaken to quantify the cross-shore sediment flux due to different frequency components. The results obtained for the cross-shore current velocity ( $u$ ) and suspended sediment concentration ( $c$ ) data records from Mullaloo Beach, presented in Figure 3, are shown in Figure 6. The instrument station was placed just outside of the breaker zone, where the seabed was flat. The mean water depth ( $h$ ) was 1.14 m, with a significant wave height ( $H_s$ ) of 0.97 m leading to a high  $H_s/h$  of 0.85.

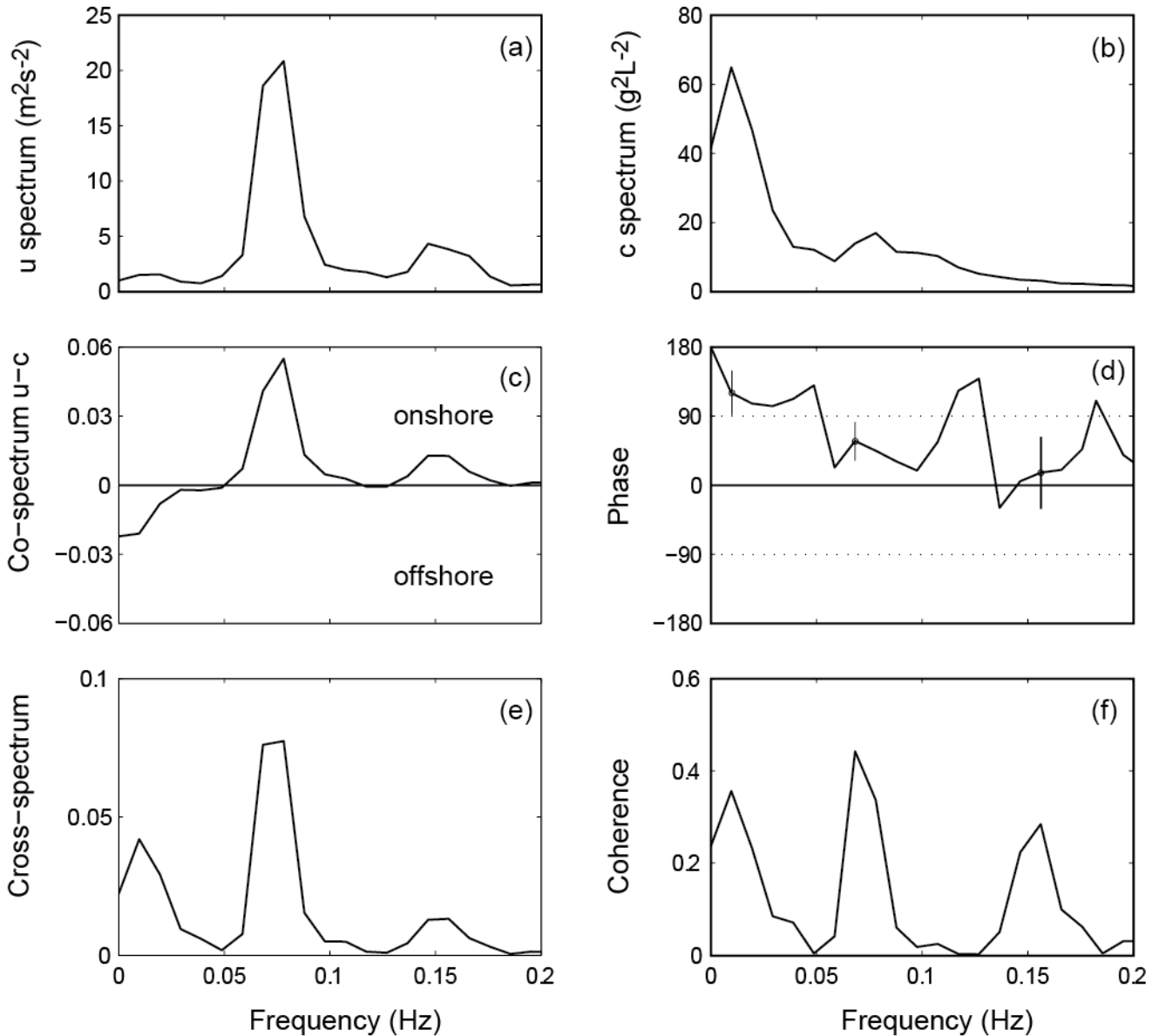
**Figure 5.** Time series of (a) cross-shore current velocity  $u$  ( $z = 0.25$  m; solid line) and the envelope function of  $u$  (thick, dashed lines); and (b) suspended sediment concentration  $c$  ( $z = 0.05$  m; solid line) and low-pass-filtered  $c$  (thick, dashed line) (just outside of the breaker line, over a flat bed, Ambakandawila Beach, Chilaw, Sri Lanka).



The auto-spectra of the cross-shore current ( $u$ ) and suspended sediment concentration ( $c$ ) (Figure 6a,b) were used to identify the dominant frequencies. The dominant peak for  $u$  was approximately 0.075 Hz, which corresponded to swell ( $\sim 13$  s). A secondary peak of about 0.15 Hz ( $\sim 7$  s) was due to the first harmonic of the swell waves; a minor peak was observed at the infragravity frequency of around 0.01 Hz (Figure 6a). The  $c$  spectrum, however, showed a low, secondary peak at the swell frequency ( $\sim 0.075$  Hz) and a distinct dominant peak at the infragravity frequency of 0.01 Hz (100 s), which corresponded to wave groups, indicating more sediment was stirred at infragravity frequencies.

The co-spectrum between the time series of  $u$  and  $c$  (suspended sediment flux in the frequency domain) (Figure 6c) showed the original finding for shoaling waves outside of the breaker zone [6]: the cross-shore sediment flux was onshore at high frequencies (swell waves) and offshore at infragravity frequencies. A minor onshore component was observed at the first harmonic of the swell waves. The same pattern was observed in most of the measurements when the instrument station was positioned just outside of the breaker line under shoaling waves over a flat bed.

**Figure 6.** The results of spectral analysis between  $u$  and  $c$ . (a) Auto-spectrum of  $u$ ; (b) auto-spectrum of  $c$ ; (c)  $c$ - $u$  co-spectrum in ( $\text{gL}^{-1}$ ) ( $\text{ms}^{-1}$ )  $\text{Hz}^{-1}$ ; (d)  $c$ - $u$  phase spectrum; (e)  $c$ - $u$  cross spectrum; (f)  $c$ - $u$  coherence spectrum (just outside of the breaker line, over a flat bed, Mullaloo Beach, Western Australia).



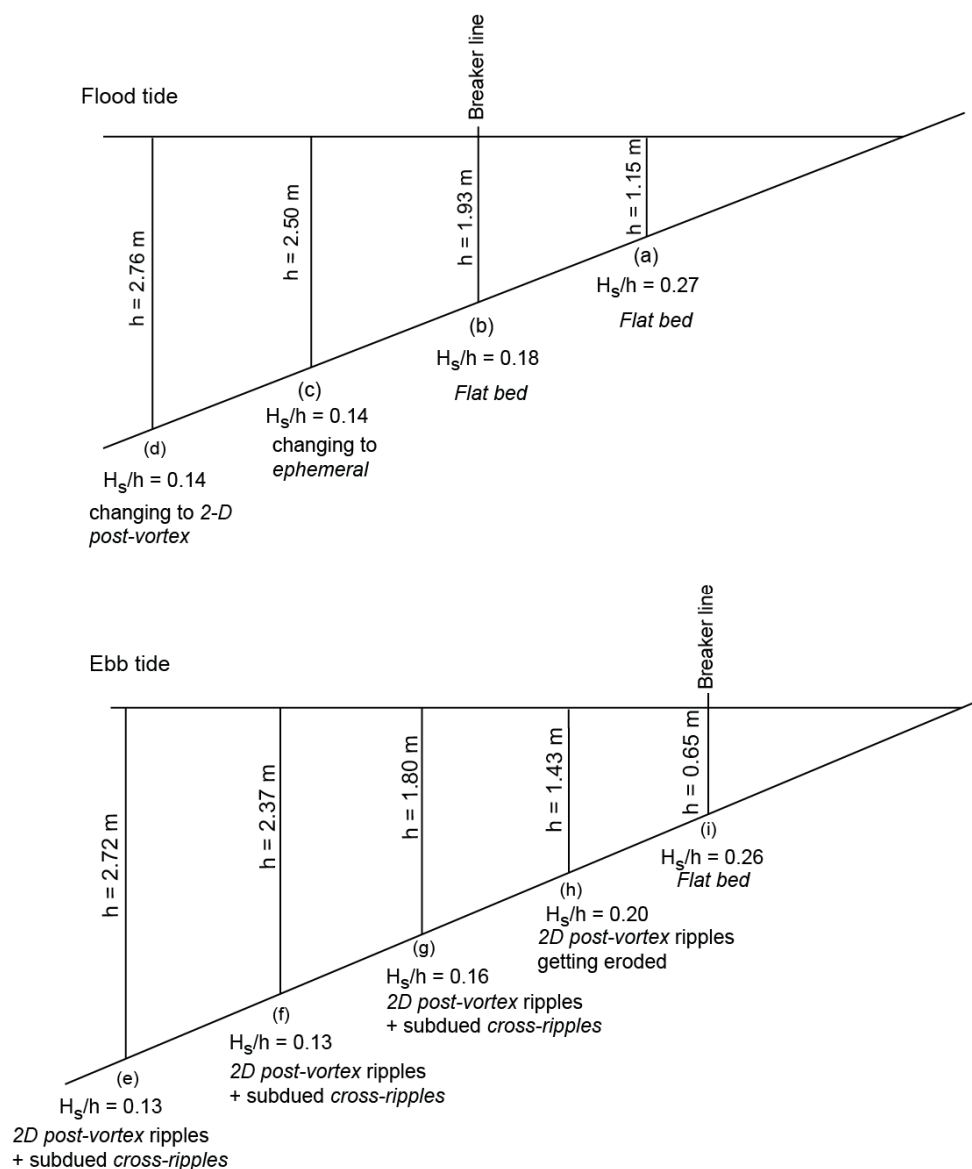
The phase lag between  $u$  and  $c$  (Figure 6d) was a direct indicator of the direction of cross-shore sediment flux. Flux was onshore if the phase lag was between  $\pm 90^\circ$  and offshore if the phase lag is outside  $\pm 90^\circ$ . At the swell and the first harmonic of the swell frequency band, the phase lag was less than  $90^\circ$ , leading to onshore flux, whereas at infragravity frequencies, the phase lag was greater than  $90^\circ$ , resulting in offshore flux. The phase spectrum at the major frequency components (Figure 6d) showed that the magnitude and direction of the co-spectral peaks at all of the three major frequency components were statistically significant at the 95% level (Figure 6d).

The cross-spectrum between  $u$  and  $c$  illustrated the gross sediment flux rates in the frequency domain (Figure 6e); strong coherence between  $u$  and  $c$  was observed at swell and infragravity frequencies, as well as the first harmonic of the swell waves (Figure 6f).

3.2.2. Temporal Variability: Tidal Cycle

At Cable Beach (Broome), data collection began during the flood tide (at around 09:40, local time) with the instrument station positioned inside of the surf zone and was completed before the onset of the sea breeze (at around 14:00), when the instrument station was again inside of the surf zone during the ebb tide. The breaker line migrated past the instrument station during the flood tide (at around 10:05) and back again during the ebb tide (at around 13:30). The spectral analysis was conducted for nine time series records of 8192 data points, covering different flow and bed conditions. The positioning of the instrument station with respect to the breaker line for each data set is presented in Figure 6, which includes details of the prevailing conditions for the flood (Figure 7a) and ebb (Figure 7b) tides.

**Figure 7.** Schematic diagram of the beach face and the positioning of the instrument station with respect to the varying water level due to the tidal cycle, Cable Beach, Broome, Western Australia. The instrument station was maintained at one place, whilst the water level changed due to the tide. Note the different scales along the y-axis).



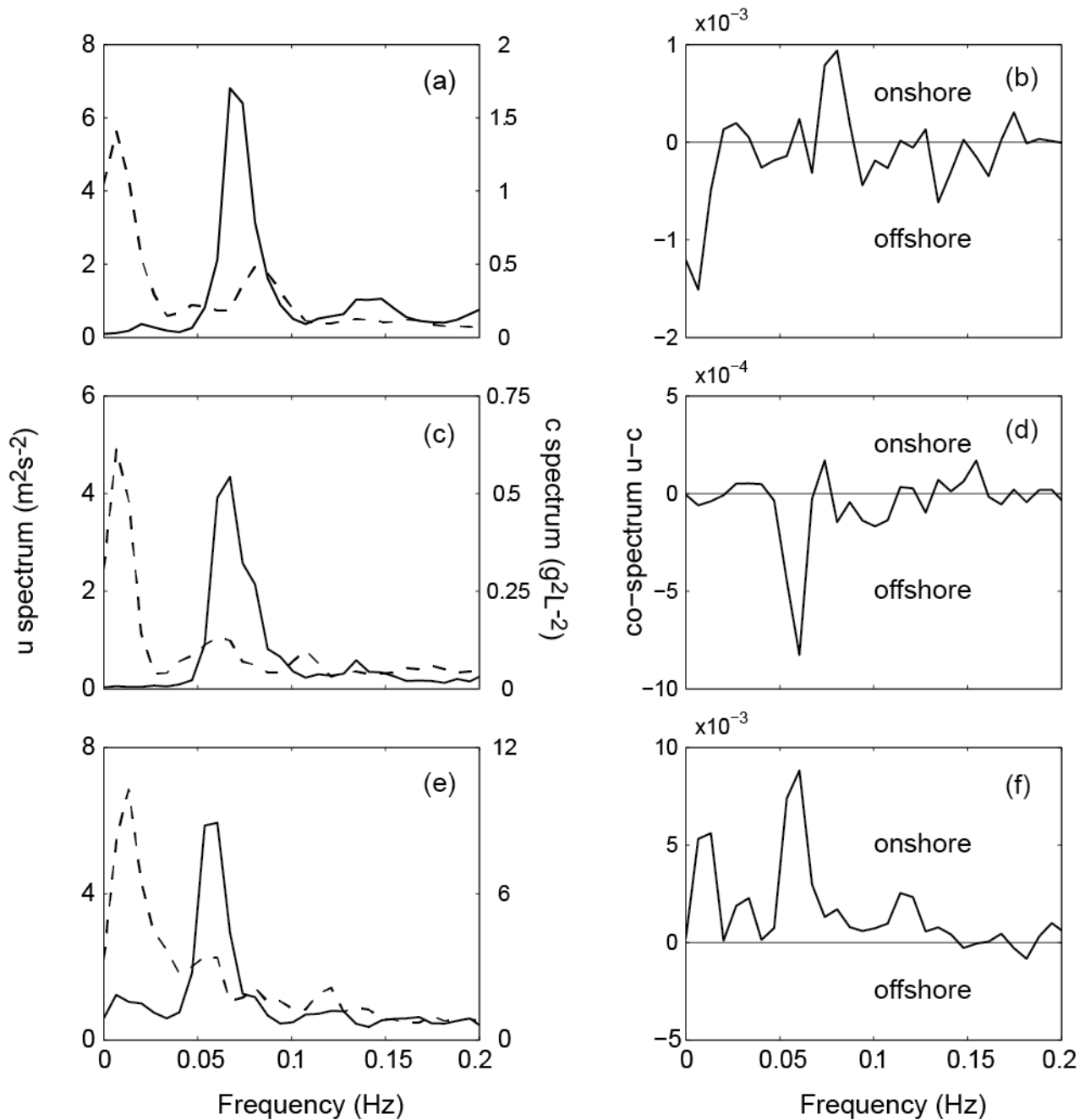
Two ripple types were observed during the measurement period in Broome: ephemeral post-vortex and permanent post-vortex ripples. At around 10:40 local time, after the breaker line had migrated past the instrument station during the rising tide, two-dimensional ephemeral ripples were observed in a mean water depth of about 2.5 m. The ripple lengths ( $\lambda$ ) were 0.06–0.08 m, and the ripple heights ( $\eta$ ) were a few millimetres. The ripples were called ephemeral, because they were not always present; they were washed away during the larger waves of the wave groups and re-formed by the smaller waves. Two-dimensional permanent post-vortex ripples, with ripple lengths similar to ephemeral ripples and ripple heights of around 0.005 m, were observed between 11:10 and 13:10 local time. Both ripple types were called post-vortex, because the ripple steepness ( $\eta/\lambda$ ) was less than 0.1 [43].

Spectral analysis results for data sets when the instrument station was just outside of the breaker line ( $h = 1.93$  m), farther outside of the breaker line ( $\sim 110$  m,  $h = 2.72$  m) and back inside of the surf zone ( $h = 0.65$  m) are presented in Figure 8a–f, respectively. Cross-shore current velocity ( $u$ ) peaked at the swell wave frequency throughout the measurement period, with minor peaks at low frequencies and the first harmonic of the swell waves (Figure 8a,c,d). When the instrument station was farther offshore of the moving shoreline, however, the low frequency component disappeared (Figure 8c). The suspended sediment concentration ( $c$ ) was dominant at infragravity frequencies (Figure 8a,c,d), suggesting that wave groups suspended more sediments than swell waves.

The suspended sediment flux due to swell waves was onshore just outside of the surf zone (Figure 8b), offshore when the instrument station was farther offshore of the breaker line (Figure 8d) and onshore again inside of the surf zone (Figure 7f). At infragravity frequencies, the sediment flux was offshore, outside of the surf zone (stronger closer to the breaker line) and onshore, inside of the surf zone. The cross-shore sediment flux values were greater during the ebb tide, especially when the instrument station was inside of the surf zone. Masselink and Pattiaratchi [34], with the same data set, showed that the suspended sediment concentration was greater during the ebb tide than during the flood tide; Davidson *et al.* [15] also observed this in their study. Statistical significance tests based on the 95% confidence interval in the phase spectrum [15] were conducted for each data set, as shown in Figure 5d. The tests revealed that spectral peaks observed at both infragravity and swell frequencies were statistically significant (data not shown).

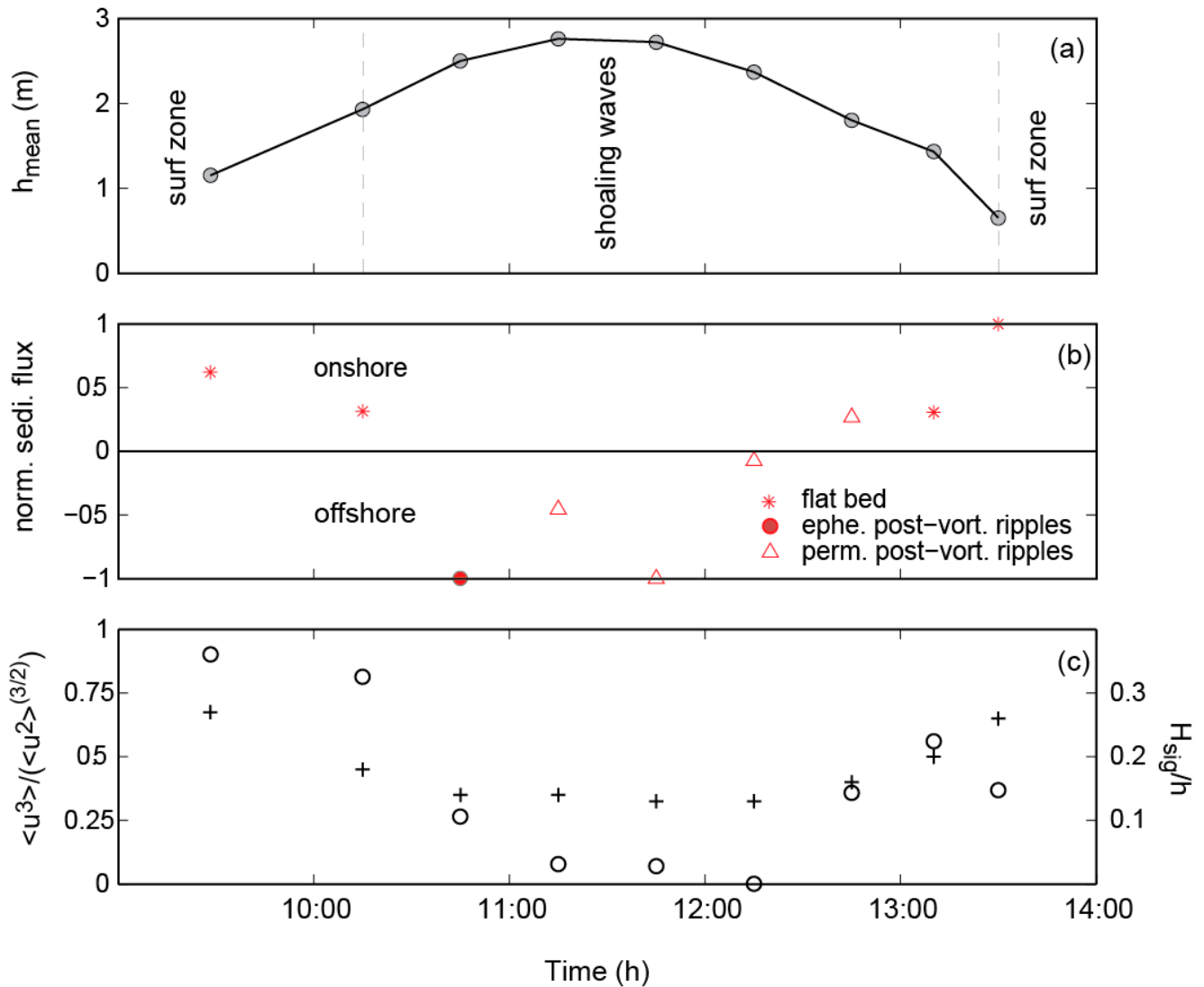
The net cross-shore suspended sediment flux at the swell frequency band ( $0.04 \text{ Hz} < \text{frequency} < 0.1 \text{ Hz}$ ) was estimated and normalised by the total (absolute) cross-shore flux within the same frequency range. These values were obtained from the area under the co-spectrum; the frequency range was chosen using the spectral valleys observed in the corresponding  $u$  spectrum. The variation of normalised net cross-shore sediment flux with the mean water depth (tide level) (Figure 9a) is presented in Figure 9b. Net sediment flux due to swell waves was onshore inside and just outside of the surf zone and offshore, farther outside of the surf zone. Moreover, when the seabed was flat, the sediment flux was observed onshore, whereas it reversed to offshore over rippled beds. The net sediment flux was onshore over a rippled bed only for the data set starting at 12:45. At this point, however, the co-spectrum between  $u$  and  $c$  was bi-directional; the ripples began to wash away with the lowering tide. It should be noted that other surrounding conditions also changed during this time. The ratio of significant wave height to mean water depth ( $H_s/h$ ) was greater close to the breaker line; net sediment flux due to swell waves was onshore under greater  $H_s/h$  and offshore under lower  $H_s/h$  (Figure 9c).

**Figure 8.** Auto-spectra of  $u$  (solid line) and  $c$  (dashed line) and co-spectrum between  $u$  and  $c$  for time series records starting at: (a,b) 10:15 (just outside of the surf zone, over a flat bed, during flood tide;  $h_m = 1.93$  m); (c,d) 11:45 (~110 m offshore of the breaker line, over permanent post-vortex ripples;  $h_m = 2.72$  m); (e,f) 13:30 (inside of the surf zone, over a flat bed, during ebb tide;  $h_m = 0.65$  m); Cable Beach, Broome, Western Australia.



The normalised velocity skewness ( $\langle u^3 \rangle / \langle u^2 \rangle^{3/2}$ ) for the swell frequency band (frequency  $> 0.04$  Hz) was calculated for each data set, as Russell and Huntley [28] explained, and plotted with the varying tide level in Figure 9c (velocity skewness is considered positive in the onshore direction and negative in the offshore direction). The suspended sediment flux at the swell frequency band was onshore when the normalised velocity skewness was high and offshore when the skewness was low but, still positive (Figure 9b,c).

**Figure 9.** Variation of (a) the mean water depth; (b) the normalised net cross-shore suspended sediment flux due to swell waves (ephe. post-vort: ephemeral post vortex; perm. post-vort: permanent post vortex); (c) the normalised velocity skewness (o) and the ratio of significant wave height to water depth (+) with time; Cable Beach, Broome, Western Australia.

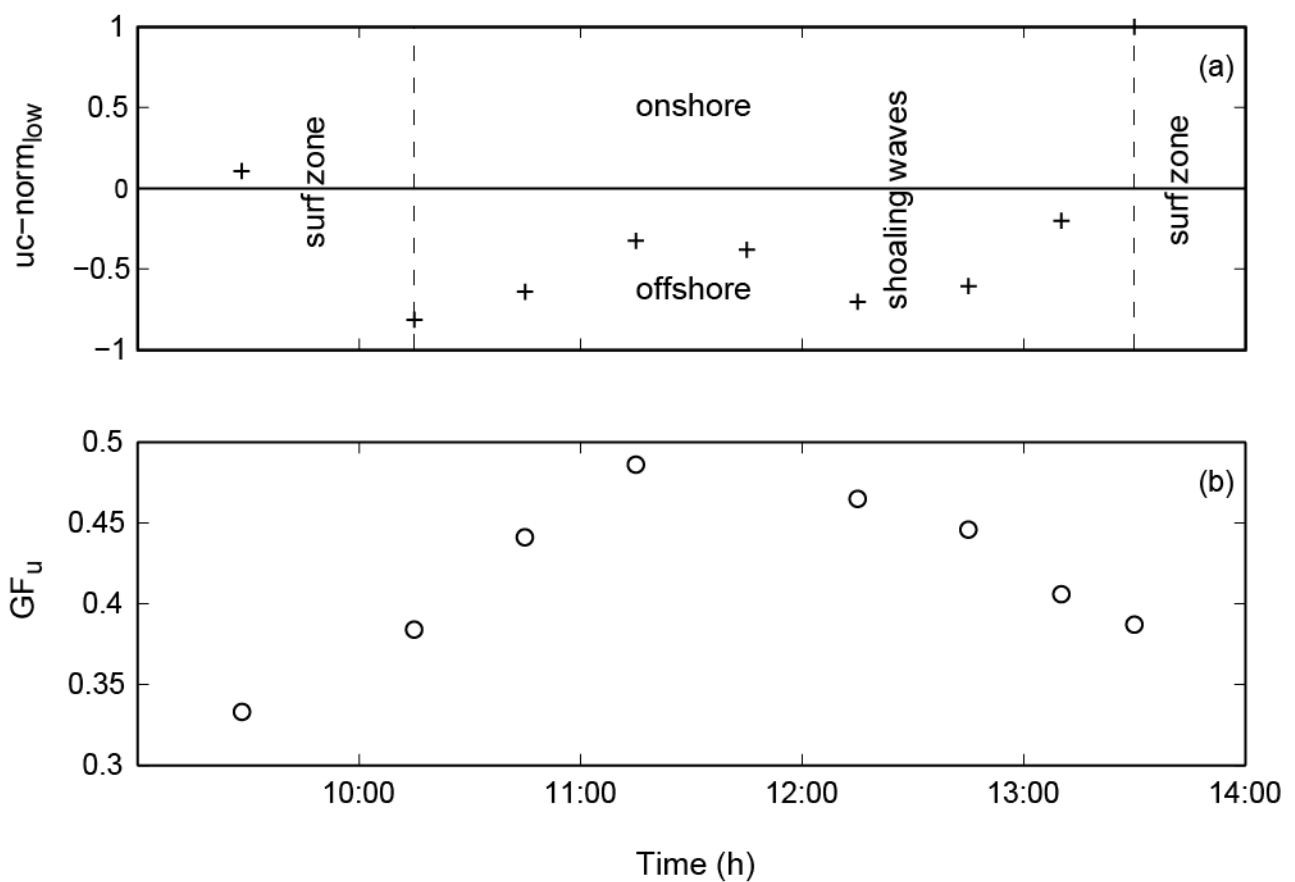


The normalised net cross-shore sediment flux calculated for the infragravity frequency band (<math><0.03\text{ Hz}</math>) was offshore outside of the surf zone and onshore, inside of the surf zone (Figure 10a). The results are similar to those found by Aagaard and Greenwood [24]. The wave groupiness factor was computed according to List [40]; it was greater when the instrument station was farther outside of the breaker zone and relatively less inside of the surf zone, as the group structure was altered during wave breaking [10].

3.2.3. Spatial Variability: Inside and Outside of the Surf Zone

The data obtained from a series of field measurements undertaken at Ambakandawila Beach (Chilaw) (Figure 1c) were analysed to investigate the variation in cross-shore sediment flux in the frequency domain. The measurements at this location (Figure 5) were obtained around the breaker line, where the waves broke almost on the beach face with a narrow surf zone. The breaking waves were surging/plunging, which the calculations of the Iribarren number supported. The seabed remained flat throughout.

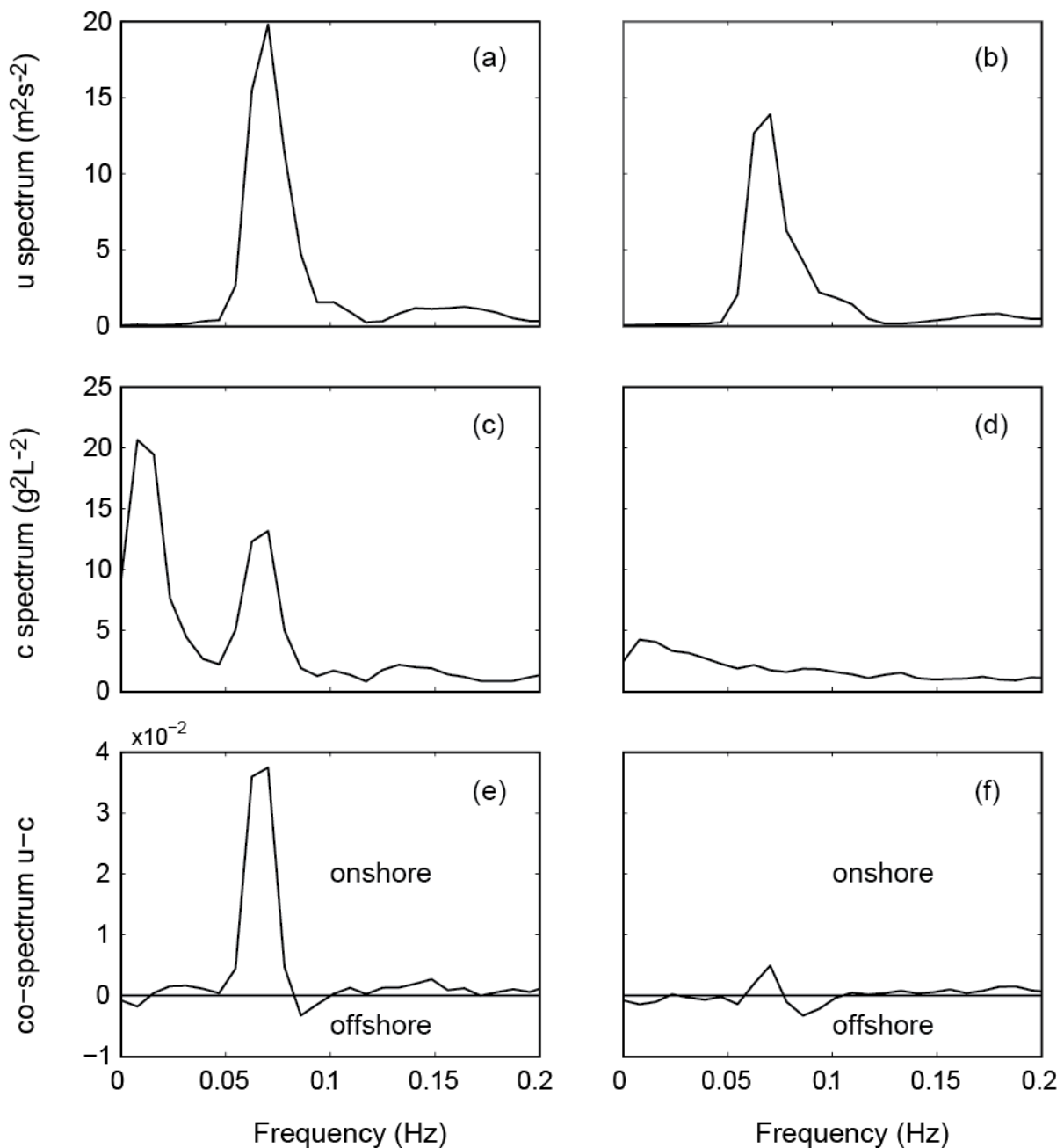
**Figure 10.** Variation of (a) normalised net suspended sediment flux (+) due to infragravity frequency waves; (b) wave groupiness factor (o) with time; Cable Beach, Broome, Western Australia.



Spectral analysis results were obtained for two data sets (just under and 2 m inside of the breaker line), which produced different outcomes (Figure 11). The cross-shore current velocity ( $u$ ) spectrum showed a dominant peak at the swell frequency band, with small infragravity frequency oscillations in either data set (Figure 11a,b); however, the wave energy reduced during the wave breaking (Figure 11a,b). The suspended sediment concentration ( $c$ ) showed dominant peaks at infragravity frequencies for both data sets. At the swell frequency band, a distinct peak was observed under the breaking waves (Figure 11c), whereas no distinct peak was observed inside of the breaker line (Figure 11d). Further, the suspended sediment concentration ( $c$  spectrum) reduced during the wave breaking (Figure 11c,d). The cross-shore suspended sediment flux under the breaking waves showed a strong onshore component at the swell frequency band and a weaker offshore component at

infragravity frequencies (Figure 11e); just after the breaker line, the magnitude of sediment flux reduced, showing a smaller bi-directional component at the swell frequency band and a negligible offshore component at infragravity frequencies (Figure 11f). The net suspended sediment flux at the swell frequency band, however, was offshore.

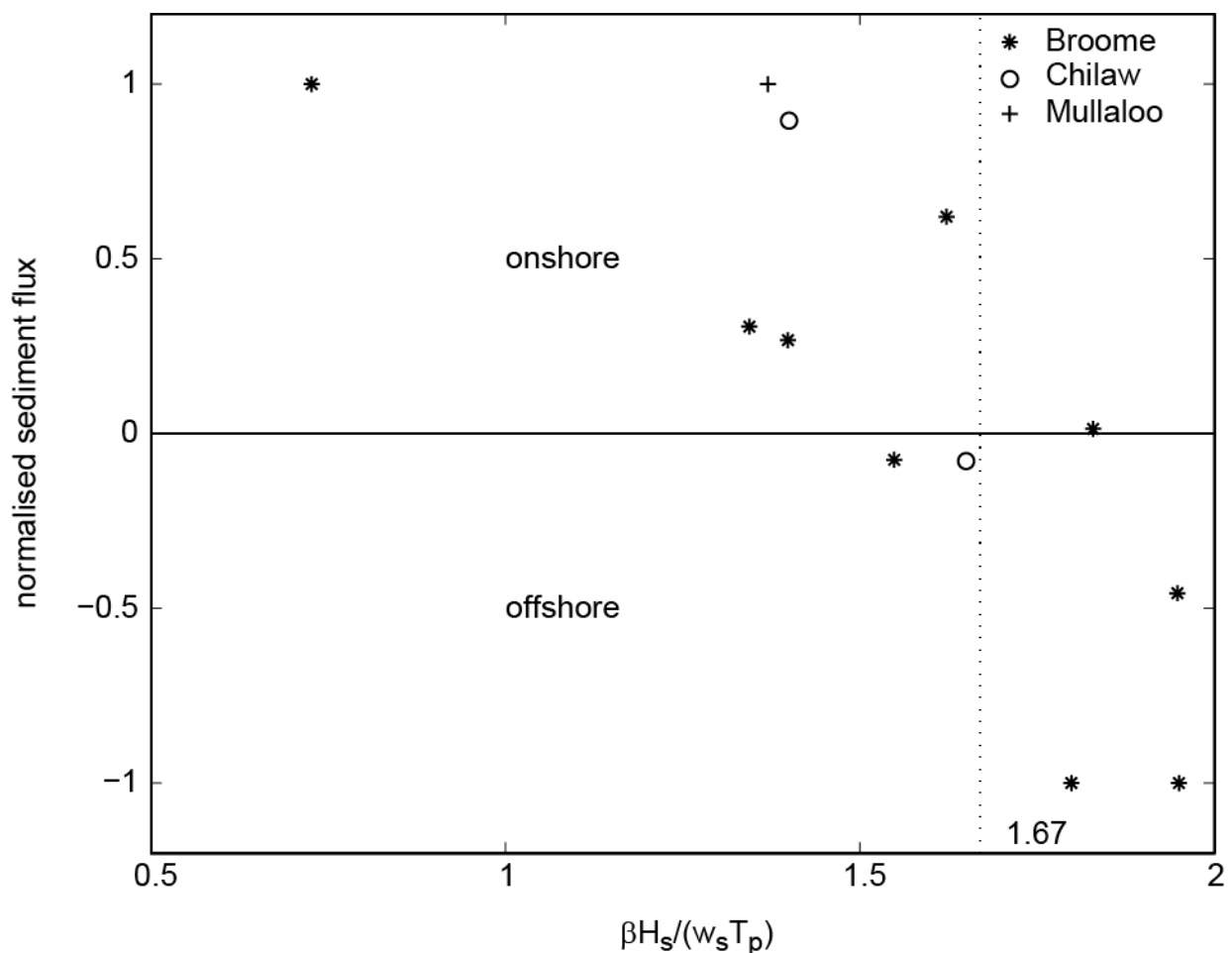
**Figure 11.** Results of spectral analysis between  $u$  and  $c$  (a,c,e) just under the surging/plunging breaker line: (a)  $u$  spectrum, (c)  $c$  spectrum, (e)  $c$ - $u$  co-spectrum; and (b,d,f) 2 m shoreward of the breaker line: (b)  $u$  spectrum, (d)  $c$  spectrum, (f)  $c$ - $u$  co-spectrum; Ambakandawila Beach, Chilaw, Sri Lanka.



3.2.4. Variation with the Dean Number

The variation of normalised cross-shore suspended sediment flux due to swell waves with the Dean number [41] is presented in Figure 12. The Dean number ( $D$ ) indicates that the sediment flux should be onshore when  $D < 1.67$  and offshore when  $D > 1.67$  (Equations (1) and (2)). The results obtained from the present study are in agreement, with the sediment flux being mainly onshore when  $D < 1.67$  and offshore when  $D > 1.67$  (Figure 12). A few points did not agree; however, at these points, the normalised sediment flux was close to zero, where the sediment flux component at the swell band was bi-directional (e.g., Figure 8d).

**Figure 12.** Variation of normalised net cross-shore suspended sediment flux with the Dean number ( $\beta H_s / (w_s T_p)$ ).



**4. Discussion**

A series of field measurements, covering different hydrodynamic and morphological conditions, was conducted to investigate the factors influencing the magnitude and direction of cross-shore suspended sediment flux, close to the seabed (0.05 m), in nearshore environments.

The results from all of the measurement sites indicated a significant relationship between the wave groups and the suspended sediment concentration. This affirmed the well-established assumption that wave groups are more capable than individual swell waves of stirring sediments and retaining

them in suspension [9,10,12]. This phenomenon was observed in the presence and absence of ripples during this study, which suggested that although the presence of ripples could cause higher suspension events [12,17,44], hydrodynamics within the wave groups alone caused the increased suspension events [15,16]. Vincent *et al.* [12], Osborne and Greenwood [10] and Villard and Osborne [17] also proposed explanations for this phenomenon.

The direction and magnitude of cross-shore sediment flux in the frequency domain appeared to vary at different locations under various conditions. Following are descriptions of the identified features.

#### 4.1. Cross-Shore Location

For most of the measurements obtained just outside of the surf zone over a flat bed, the suspended sediment flux was onshore at swell wave frequencies (swell, wind waves) and offshore at lower frequencies (corresponding to wave groups), which agreed with Huntley and Hanes's [6] widely accepted finding. Increased velocity skewness towards the wave propagation direction as the waves shoaled might have forced the suspended sediment onshore [18,23]. Further, it has been found that under near-breaking and breaking waves, large fluid accelerations skewed towards shore, suspending more sediments [9,10,16,44]. These coincide with the onshore phase of the cross-shore velocity, causing onshore sediment flux [45]. Moreover, the large waves in the groups suspend more sediment, which, in turn, coincides with the trough of the group-bound long wave [20] moving sediment offshore at infragravity frequencies [21,22].

Inside of the surf zone, similar to shoaling waves just outside, the sediment flux at the swell band was usually towards shore, although the infragravity frequency component varied [24]. This might have been because wave groups were destroyed and then the group-bound long wave was released during the wave breaking [23].

In some cases (e.g., Chilaw), however, the magnitude of the suspended sediment flux just inside of the breaker line reduced (by order of magnitude) relative to the flux just under the breaking waves (Figure 11). The breaker type was surging/plunging. In contrast, in Broome the sediment flux increased inside of the breaker zone, where spilling breakers were evident. The strong sediment flux just under the breaker line (Figure 11e) might have been due to turbulence vortices generated by wave breakers; these vortices might not have reached 2 m inside of the plunge point. The increased uniformity in the suspended sediment concentration after the wave breaking, as the wave structure was destroyed, because of surging/plunging, might have caused the bi-directionality in the co-spectrum [23].

In Broome, where the large tidal range caused the instrument station position to move with respect to the moving breaker line, the direction and magnitude of cross-shore suspended sediment flux varied. When the instrument station was inside and just outside of the surf zone, with a flat bed, the suspended sediment flux due to swell waves was onshore, as was observed throughout the study. Conversely, when the instrument station was farther offshore, the suspended sediment flux was predominantly offshore (Figure 9b). However, other factors, such as bed forms and velocity skewness, which also changed along with the location with respect to the moving breaker line, could well have influenced the suspended sediment flux.

#### 4.2. Bed Ripples

In Broome, the seabed configuration changed with the varying tide level. The seabed was flat when the instrument station was inside and just outside of the surf zone during the rising tide. Ephemeral post-vortex and permanent post-vortex ripples were present, while the instrument station was farther offshore of the breaker line (around high tide). The seabed was flat again when the instrument station was back in the surf zone during the ebb tide (Figure 9b). The suspended sediment flux due to swell waves followed this pattern; it was onshore when the seabed was flat and predominantly offshore when the bed was rippled (Figure 9b).

Inman and Bowen [46] first proposed an explanation for sediment moving against the direction of wave propagation over a rippled bed: when a skewed wave propagates over vortex ripples, during the relatively strong onshore phase, a vortex is formed on the leeside of the ripple and remains trapped until the flow reverses; during the weaker offshore phase, the vortex shoots up into the water column, carrying a cloud of sediment. Simultaneously, the offshore phase moves this sediment cloud back. This breakdown was explained for vortex ripples, whereas the ripples observed during this study were clearly post-vortex (steepness less than 0.1) [43].

The offshore sediment flux due to swell waves over less steep post-vortex ripples, however, has been observed in the past [23,27,47]. Davidson *et al.* [15] also observed offshore flux at the swell band over ripples, but the ripple geometry was not measured, so it was uncertain whether the ripples were vortex or post-vortex.

No clear difference in the direction of suspended sediment flux due to swell waves could be identified between ephemeral post-vortex and permanent post-vortex ripples, as the sediment flux was predominantly offshore over both types.

#### 4.3. Velocity Skewness ( $\langle u^3 \rangle / \langle u^2 \rangle^{3/2}$ )

As the location of measurement location changed with the rising/falling tide, the normalised velocity skewness due to the incident swell waves also changed (Figure 9c). The normalised net sediment flux was onshore when the velocity skewness was high, whereas offshore flux was observed under lower skewness values, although the skewness had been positive throughout. Russell and Huntley [28] predicted onshore transport associated with swell wave skewness under high energy conditions both inside and outside of the surf zone where the seabed was flat. Increased velocity skewness in the wave propagation direction as waves shoal could force the suspended sediment onshore [18,23]. Russell and Huntley [28] further suggested that under low energy conditions (e.g., in the presence of ripples), the velocity skewness might not predict the direction of cross-shore sediment transport. The results of the present study agreed with this, as offshore sediment flux was observed under low energy conditions in the presence of ripples when the velocity skewness was still positive (Figure 9b,c).

#### 4.4. Dean Number ( $D$ )

The variation in the direction of cross-shore suspended sediment flux due to swell waves with the Dean number agreed with Dean and Dalrymple's [44] explanation: it was onshore when  $D < 1.67$

and offshore when  $D > 1.67$  (Figure 12). This was remarkable, given that Dean and Dalrymple's explanation did not account for parameters, such as ripples or velocity skewness; it was based on whether the sediment particles, suspended by each wave, would settle before or after the flow reversed and, hence, transport onshore or offshore. However, it should be noted that this finding is based on measurements undertaken on the swell (and wave group)-dominated beaches presented here.

Further investigations of the changes in the above-discussed parameters would enable a better understanding of cross-shore suspended sediment transport in nearshore environments. A detailed study of the direction and magnitude of cross-shore suspended sediment flux over different ripple types would be particularly useful. A numerical model that accommodates all of these factors could be an excellent tool to investigate the influence of these factors independently (see, for example, [48]).

## 5. Conclusions

A series of field measurements of hydrodynamics and sediment suspension, together with bed topography, was collected at several nearshore locations to investigate the influence of infragravity waves, ripple type and location relative to the breaker line on cross-shore suspended sediment flux close to the bed. The following features were identified:

- (a) A significant correlation between wave groups and suspended sediment concentration was observed at all of the measurement sites, confirming the well-established assumption that wave groups are more capable than incident swell waves of equal amplitude of suspending sediments. This correlation was observed in the presence and absence of ripples.
- (b) The direction and magnitude of suspended sediment flux varied depending on the measurement location with respect to the breaker line; however, other parameters, such as bed ripples and velocity skewness, could have influenced this.
- (c) At infragravity frequencies, the suspended sediment flux was mainly offshore outside of the surf zone (due to the combined action of wave groups and the group-bound long wave), while it varied inside of the surf zone. The wave groupiness factor was greater farther offshore of the surf zone and was relatively low inside of the surf zone.
- (d) The direction and magnitude of the suspended sediment flux inside of the breaker line changed with the breaker type.
- (e) Offshore suspended sediment flux due to swell waves was observed over less steep post-vortex ripples.
- (f) At the swell frequency band, onshore sediment flux was observed when the normalised velocity skewness was high; offshore flux was observed when the skewness was lower, but still positive, suggesting the influence of other parameters, such as ripples and grain size [28].
- (g) Suspended sediment flux due to swell waves was predominantly onshore when the Dean number was less than 1.67 and offshore when the Dean number was greater than 1.67. This agreed with Dean and Dalrymple's [44] simple hypothesis, although it did not account for the influence of bed ripples or wave asymmetry.

## Acknowledgments

We would like to thank Gerd Masselink for leading the field campaign in Broome, assisted by Rob Brander, Jeff Doucette, Michael Hughes, Aart Kroon, Guilherme Lessa, Dave Mitchell and Jypsy. The data from Chilaw were collected in conjunction with the Lanka Hydraulic Institute and funded by the Ministry of Fisheries and Aquatic Resources (Sri Lanka). Jeff Doucette and Nalin Wikramanayake provided useful comments on the manuscript. This paper is in memory of Samantha Kularatne who tragically passed away in September 2009.

## Author Contributions

Conducted the field-work: CP. Analysed the data: SK. Wrote the paper: SK, CP.

## Conflicts of Interest

The authors declare no conflict of interest.

## References

1. Masselink, G.; Pattiaratchi, C. The effect of sea breeze on beach morphology, surf zone hydrodynamics and sediment resuspension. *Mar. Geol.* **1998**, *146*, 115–135.
2. Yates, M.L.; Guza, R.T.; O'Reilly, W.C. Equilibrium shoreline response: Observations and modeling. *J. Geophys. Res.* **2009**, *114*, C09014; doi:10.1029/2009JC005359.
3. Hanson, H.; Larson, M.; Kraus, N.C. Calculation of beach change under interacting cross-shore and longshore processes. *Coast. Eng.* **2010**, *57*, 610–619.
4. Sternberg, R.W.; Shi, N.C.; Downing, J.P. Continuous measurements of suspended sediment. In *Nearshore Sediment Transport*; Seymour, R.J., Ed.; Springer: New York, NY, USA, 1989; pp. 231–257.
5. Baldock, T.E.; Alsina, J.A.; Caceres, I.; Vicinanza, D.; Contestabile, P.; Power, H.; Sanchez-Arcilla, A. Large-scale experiments on beach profile evolution and surf and swash zone sediment transport induced by long waves, wave groups and random waves. *Coast. Eng.* **2011**, *58*, 214–227.
6. Huntley, D.A.; Hanes, D.M. Direct measurement of suspended sediment transport. In *Coastal Sediments '87*, Proceedings of a Specialty Conference on Advances in Understanding of Coastal Sediment Processes, New Orleans, LA, USA, 12–14 May 1987; Kraus, N.C., Ed.; American Society of Civil Engineers: New York, NY, USA, 1987; pp. 723–737.
7. Brenninkmeyer, B.M. *In situ* measurements of rapidly fluctuating, high sediment concentrations. *Mar. Geol.* **1976**, *20*, 117–128.
8. Sternberg, R.W.; Shi, N.C.; Downing, J.P. Field investigations of suspended sediment transport in the nearshore zone. In *Coastal Engineering (1984)*, Proceedings of the International Nineteenth Coastal Engineering Conference, Houston, TX, USA, 3–7 September 1984; Edge, B.L., Ed.; American Society of Civil Engineers: New York, NY, USA, 1984; pp. 1782–1798.
9. Hanes, D.M.; Huntley, D.A. Continuous measurements of suspended sand concentration in a wave dominated nearshore environment. *Cont. Shelf Res.* **1986**, *6*, 585–596.

10. Osborne, P.D.; Greenwood, B. Sediment suspension under waves and currents: Time scales and vertical structure. *Sedimentology* **1993**, *40*, 599–622.
11. Hanes, D.M. Suspension of sand due to wave groups. *J. Geophys. Res.* **1991**, *96*, 8911–8915.
12. Vincent, C.E.; Hanes, D.M.; Bowen, A.J. Acoustic measurements of suspended sand on the shoreface and the control of concentration by bed roughness. *Mar. Geol.* **1991**, *96*, 1–18.
13. Williams, J.J.; Rose, C.P.; Thorne, P.D. Role of wave groups in resuspension of sandy sediments. *Mar. Geol.* **2002**, *183*, 17–29.
14. Kularatne, S.; Pattiaratchi, C.B. Turbulent kinetic energy and sediment resuspension due to wave groups. *Cont. Shelf Res.* **2008**, *28*, 726–736.
15. Davidson, M.A.; Russell, P.E.; Huntley, D.A.; Hardisty, J. Tidal asymmetry in suspended sand transport on a macrotidal intermediate beach. *Mar. Geol.* **1993**, *110*, 333–353.
16. Hay, A.E.; Bowen, A.J. Coherence scales of wave-induced suspended sand concentration fluctuations. *J. Geophys. Res.* **1994**, *99*, 12749–12766.
17. Villard, P.V.; Osborne, P.D. Visualization of wave-induced suspension patterns over two-dimensional bedforms. *Sedimentology* **2002**, *49*, 363–378.
18. Doering, J.C.; Bowen, A.J. Wave-induced flow and nearshore suspended sediment. In *Coastal Engineering (1988)*, Proceedings of the International Twenty-first Coastal Engineering Conference, Coata del Sol-Malaga, Spain, 20–25 June 1988; Edge, B.L., Ed.; American Society of Civil Engineers: New York, NY, USA, 1989; pp. 1452–1463.
19. Osborne, P.D.; Greenwood, B. Frequency dependent cross-shore suspended sediment transport. 1. A non-barred shoreface. *Mar. Geol.* **1992**, *106*, 1–24.
20. Longuet-Higgins, M.S.; Stewart, R.W. Radiation stresses in water waves: A physical discussion, with applications. *Deep Sea Res.* **1964**, *11*, 529–562.
21. Larsen, L.H. A new mechanism for seaward dispersion of midshelf sediments. *Sedimentology* **1982**, *29*, 279–283.
22. Shi, N.C.; Larsen, L.H. Reverse sediment transport induced by amplitude-modulated waves. *Mar. Geol.* **1984**, *54*, 181–200.
23. Osborne, P.D.; Greenwood, B. Frequency dependent cross-shore suspended sediment transport. 2. A barred shoreface. *Mar. Geol.* **1992**, *106*, 25–51.
24. Aagaard, T.; Greenwood, B. Suspended sediment transport and morphological response on a dissipative beach. *Cont. Shelf Res.* **1995**, *15*, 1061–1086.
25. Osborne, P.D.; Vincent, C.E. Dynamics of large and small scale bedforms on a macrotidal shoreface under shoaling and breaking waves. *Mar. Geol.* **1993**, *115*, 207–226.
26. Osborne, P.D.; Vincent, C.E. Vertical and horizontal structure in suspended sand concentrations and wave-induced fluxes over bedforms. *Mar. Geol.* **1996**, *131*, 195–208.
27. Doucette, J.S. The distribution of nearshore bedforms and effects on sand suspension on low-energy, micro-tidal beaches in southwestern Australia. *Mar. Geol.* **2000**, *165*, 41–61.
28. Russell, P.E.; Huntley, D.A. A cross-shore transport “shape function” for high energy beaches. *J. Coast. Res.* **1999**, *15*, 198–205.
29. Aagaard, T.; Nielsen, J.; Greenwood, B. Suspended sediment transport and nearshore bar formation on a shallow intermediate-state beach. *Mar. Geol.* **1998**, *148*, 203–225.

30. Conley, D.C.; Beach, R.A. Cross-shore sediment transport partitioning in the nearshore during a storm event. *J. Geophys. Res.* **2003**, *108*, doi:10.1029/2001JC001230.
31. Pattiaratchi, C.B. Coastal tide gauge observations: Dynamic processes present in the Fremantle record. In *Operational Oceanography in the 21st Century*; Schiller, A., Brassington, G.B., Eds.; Springer: Heidelberg, Germany, **2011**; pp. 185–202.
32. Pattiaratchi, C.; Hegge, B.; Gould, J.; Eliot, I. Impact of sea-breeze activity on nearshore and foreshore processes in southwestern Australia. *Cont. Shelf Res.* **1997**, *17*, 1539–1560.
33. Masselink, G.; Pattiaratchi, C.B. Seasonal changes in beach morphology along the sheltered coastline of Perth, Western Australia. *Mar. Geol.* **2001**, *172*, 243–263.
34. Masselink, G.; Pattiaratchi, C. Tidal asymmetry in sediment resuspension on a macrotidal beach in northwestern Australia. *Mar. Geol.* **2000**, *163*, 257–274.
35. Pattiaratchi, C.; Masselink, G.; Wikramanayake, N. Sea breeze effects on coastal processes. In Proceedings of the Fifth International Conference on Coastal and Port Engineering in Developing Countries (COPEDEC V), Cape Town, South Africa, 16–17 April 1999; Council for Scientific and Industrial Research: Cape Town, South Africa, **1999**; pp. 37–48.
36. Foote, Y.; Russell, P.E.; Huntley, D.A.; Sims, P. Energetics prediction of frequency-dependent suspended sand transport rates on a macrotidal beach. *Earth Surf. Process. Landf.* **1998**, *23*, 927–941.
37. Ludwig, K.A.; Hanes, D.M. A laboratory evaluation of optical backscatterance suspended solids sensors exposed to sand-mud mixtures. *Mar. Geol.* **1990**, *94*, 173–179.
38. Bendat, J.S.; Piersol, A.G. *Random Data: Analysis and Measurement Procedures*; Wiley-Interscience: New York, NY, USA, 1986.
39. Jenkins, G.M.; Watts, D.G. *Spectral Analysis and Its Applications*; Holden-Day: San Francisco, CA, USA, 1968; p. 525.
40. List, J.H. Wave groupiness variations in the nearshore. *Coast. Eng.* **1991**, *15*, 475–496.
41. Dean, R.G. Heuristic models of sand transport in the surf zone. In *Proceedings of the Conference on Engineering Dynamics in the Surf Zone*; American Society of Civil Engineers: New York, NY, USA, 1973; pp. 208–214.
42. Dean, R.G.; Dalrymple, R.A. *Coastal Processes with Engineering Applications*; Cambridge University Press: New York, NY, USA, 2002; p. 475.
43. Clifton, H.E.; Dingler, J.R. Wave-formed structures and paleoenvironmental reconstruction. *Mar. Geol.* **1984**, *60*, 165–198.
44. Nielsen, P. *Coastal Bottom Boundary Layers and Sediment Transport*; Advanced Series on Ocean Engineering; World Scientific: Singapore, Singapore, 1992; Volume 4, p. 324.
45. Elgar, S.; Guza, R.T.; Freilich, M.H. Eulerian measurements of horizontal accelerations in shoaling gravity waves. *J. Geophys. Res.* **1988**, *93*, 9261–9269.
46. Inman, D.L.; Bowen, A.J. Flume experiments on sand transport by waves and currents. In *Coastal Engineering (1962)*, Proceedings of the eighth International Coastal Engineering Conference, Mexico City, Mexico, 26–29 November 1962; Edge, B.L., Ed.; American Society of Civil Engineers: New York, NY, USA, 1963; pp. 137–150.
47. Brander, R.W.; Greenwood, B. Bedform roughness and the re-suspension and transport of sand under shoaling and breaking waves: A field study. In Proceedings of Canadian Coastal

Conference; Vancouver, BC, Canada, 4–7 May 1993. Coastal Zone Canada Association: Ottawa, Canada, 1993; pp. 587–599.

48. Kularatne, S.R.; Pattiaratchi, C.B. Numerical model study of cross-shore suspended sediment flux in the frequency domain. *Coast. Eng. J.* 2014, in review.

© 2014 by the authors; licensee MDPI, Basel, Switzerland. This article is an open access article distributed under the terms and conditions of the Creative Commons Attribution license (<http://creativecommons.org/licenses/by/3.0/>).